

RESEARCH ARTICLE | AUGUST 04 2023

# Demonstrating the high sensitivity of MoS<sub>2</sub> monolayers in direct x-ray detectors

Alberto Taffelli ; Max Heyl ; Matteo Favaro ; Sandra Dirè ; Lucio Pancheri ;  
Emil J. W. List-Kratochvil ; Alberto Quaranta ; Giovanni Ligorio 



APL Mater. 11, 081101 (2023)

<https://doi.org/10.1063/5.0151794>View  
OnlineExport  
Citation

CrossMark



**AMERICAN ELEMENTS**  
THE ADVANCED MATERIALS MANUFACTURER 

sapphire windows	Nd:YAG
spintronics	raman substrates
silver nanoparticles	perovskites
MOICVD	beta-barium borate
rare earth metals	quantum dots
osmium	scintillation Ce:YAG
refractory metals	laser crystals
anodized alumina	InAs wafers
ZnS	CdTe
perovskite crystals	transparent ceramics

yttrium iron garnet	glassy carbon
zeolites	III-IV semiconductors
nano ribbons	barium fluoride
epitaxial crystal growth	ultra high purity materials
cerium oxide polishing powder	
surface functionalized nanoparticles	
Al	C
Si	N
P	O
S	F
Cl	Ne
Kr	
cermet	transparent ceramics
nanodispersions	CIGS
MBE grade materials	thin film
OLED lighting	solar energy
growing targets	fiber optics
h-BN	deposition slugs
CVD precursors	photovoltaics
metamaterials	borosilicate glass
YBCO	superconductors
indium tin oxide	InGaAs
MgF <sub>2</sub>	rutile
diamond micropowder	optical glass



The Next Generation of Material Science Catalogs

**Now Invent.**™

[www.americanelements.com](http://www.americanelements.com)  
© 2001-2023 American Elements is a U.S. Registered Trademark

 AIP Publishing

03 November 2023 12:24:53

# Demonstrating the high sensitivity of MoS<sub>2</sub> monolayers in direct x-ray detectors

Cite as: APL Mater. 11, 081101 (2023); doi: 10.1063/5.0151794

Submitted: 24 March 2023 • Accepted: 18 July 2023 •

Published Online: 4 August 2023



View Online



Export Citation



CrossMark

Alberto Taffelli,<sup>1,a)</sup> Max Heyl,<sup>2</sup> Matteo Favaro,<sup>1</sup> Sandra Dirè,<sup>1</sup> Lucio Pancheri,<sup>1</sup> Emil J. W. List-Kratochvil,<sup>2,3</sup> Alberto Quaranta,<sup>1,4</sup> and Giovanni Ligorio<sup>2,a)</sup>

## AFFILIATIONS

<sup>1</sup> Department of Industrial Engineering, University of Trento, Via Sommarive 9, 38123 Trento, Italy

<sup>2</sup> Institute für Physik, Institute für Chemie & IRIS Adlershof, Humboldt-Universität zu Berlin, Zum Großen Windkanal 2, 12489 Berlin, Germany

<sup>3</sup> Helmholtz-Zentrum Berlin für Materialien und Energie, Hahn-Meitner-Platz 1, 14109 Berlin, Germany

<sup>4</sup> INFN - TIFPA, Via Sommarive 14, 38123 Trento, Italy

<sup>a)</sup> Authors to whom correspondence should be addressed: [alberto.taffelli@unitn.it](mailto:alberto.taffelli@unitn.it) and [giovanni.ligorio@hu-berlin.de](mailto:giovanni.ligorio@hu-berlin.de)

## ABSTRACT

Two-dimensional transition metal dichalcogenides (TMDCs) are demonstrated to be appealing semiconductors for optoelectronic applications, thanks to their remarkable properties in the ultraviolet-visible spectral range. Interestingly, TMDCs have not yet been characterized when exposed to x rays, although they would be ideal candidates for optoelectronic applications in this spectral range. They benefit from the high cross section of the constituent heavy atoms, while keeping the absorption very low, due to the ultrathin structure of the film. This encourages the development of photodetectors based on TMDCs for several applications dealing with x rays, such as radioprotection, medical treatments, and diagnosis. Given the atomic thickness of TMDCs, they can be expected to perform well at low dose measurements with minimal perturbation of the radiation beam, which is required for *in vivo* applications. In this paper, the use of TMDCs as active materials for direct x-ray detection is demonstrated, using a photodetector based on a MoS<sub>2</sub> monolayer (1L-MoS<sub>2</sub>). The detector shows a response to x rays in the range of 10<sup>1</sup>–10<sup>2</sup> keV, at dose rates as low as fractions of mGy/s. The sensitivity of 1L-MoS<sub>2</sub> reaches values in the range of 10<sup>8</sup>–10<sup>9</sup> μC Gy<sup>-1</sup> cm<sup>-3</sup>, overcoming the values reported for most of the organic and inorganic materials. To improve the x-ray photoresponse even further, the 1L-MoS<sub>2</sub> was coupled with a polymeric film integrating a scintillator based on terbium-doped gadolinium oxysulfide (Gd<sub>2</sub>O<sub>2</sub>S:Tb). The resulting signal was three times larger, enabled by the indirect x ray to visible photoconversion mechanism. This paper might pave the way toward the production of ultrathin real-time dosimeters for *in vivo* applications.

© 2023 Author(s). All article content, except where otherwise noted, is licensed under a Creative Commons Attribution (CC BY) license (<http://creativecommons.org/licenses/by/4.0/>). <https://doi.org/10.1063/5.0151794>

03 November 2023 12:24:53

The detection and monitoring of ionizing radiation (e.g., x rays, γ-rays) are essential in several applications, such as medical treatments and diagnosis, energy and nuclear physics, and in space exploration and security. Furthermore, to guarantee more reliable dose delivery in treatments as well as to monitor unwanted radiation exposures, the study of detectors based on new materials has grown largely over the past decades. Several solutions are now available in commerce, comprising ionization chambers, radiochromic films, and semiconductor (Si, Ge, Se, CdTe)-based detectors. However, there is still demand for real-time, wearable, and cheap detectors to be used for *in vivo* applications.<sup>1</sup> These needs recently led to the study of detectors based on thin semiconductors that, due to their

lower absorption, can be placed between the source and the target to monitor radiation doses without significant perturbation of the radiation field (*in vivo* dosimeters). *In vivo* dosimeters have the potential to make a significant impact on dosimetry. They have the capability to monitor tissue doses in real-time during diagnostic procedures and radiotherapeutic treatments. This advancement can reduce the risks associated with excessive exposure to ionizing radiation with respect to the use of standard dosimeters.

In addition to the requirements for semiconductor-based dosimeters (e.g., real-time response, high sensitivity, radiation hardness), materials to be used for *in vivo* dosimeters must also exhibit low radiation absorption. This is crucial to minimize the

perturbation of the radiation field. Moreover, the devices must be wearable to adapt to the body. Recently, organic semiconductors and hybrid organo-metallic materials have been considered due to their lower attenuation coefficient, tissue equivalent response to radiation, compatibility with flexible structures, and cost-effective production methods. Several detectors based on organic<sup>2–10</sup> and hybrid organic–inorganic materials<sup>11–20</sup> have been reported in the last few years showing remarkable radiation sensitivities. Alongside the positive effects of including organic materials in the devices, one major issue is associated with their degradation when exposed to the external environment.<sup>21,22</sup> It is also known that the radiation hardness of these materials is still limited and they can be exposed only to modest radiation fluences.<sup>1</sup> Furthermore, organic-based materials are characterized by low mobility values, leading to reduced charge carrier transport and ultimately poor or limited detection. Also, the low atomic number Z of organic materials leads to limited interaction probability with x rays, compared to inorganic semiconductors.

For x-ray detection, two-dimensional semiconductors, such as TMDCs, represent a convincing alternative to perform real-time radiation monitoring for *in vivo* applications. Interestingly, although TMDCs are recently gaining extraordinary attention from the scientific community for the fabrication of opto-electronic devices—to the best of our knowledge—they have not been considered yet for direct detection of electromagnetic radiation wavelengths shorter than ultraviolet (UV). TMDCs are, in fact, high Z-semiconductors made of a layer of transition metal atoms of the VI group, e.g., Mo ( $Z = 42$ ) and W ( $Z = 74$ ), sandwiched between two layers of chalcogen atoms, e.g., S, Se, and Te. Thus, TMDCs benefit from the higher cross-section of the heavy atoms, while keeping the absorption very low, due to the ultrathin structure (0.6–0.7 nm) of the film and perform better than organic materials with respect to carrier mobility.<sup>23–26</sup> As a result of their two-dimensional nature, they become direct bandgap semiconductor,<sup>27,28</sup> leading to strong light–matter interaction in the visible range (VIS).<sup>29,30</sup> This property has been widely explored for UV-VIS detection, but it can be as well exploited for the detection of x rays and help when TMDCs are combined with scintillators, increasing the detector response. Moreover, TMDCs already showed high radiation resistance<sup>31,32</sup> and do not undergo fast degradation in ambient air.<sup>33</sup> Among TMDCs, MoS<sub>2</sub> has been extensively studied due to its abundance and ease of supply. Several published works, indeed, report its employment in photodetectors for UV-VIS-NIR radiation,<sup>34,35</sup> providing also thin and flexible solutions while showing remarkable performance.

Under these premises, the aim of this paper is to demonstrate the successful employment of TMDCs as candidate materials for applications related to direct x-ray detection technology. With this in mind, we built a planar device based on MoS<sub>2</sub> monolayer (1L-MoS<sub>2</sub>), which was characterized upon exposure to x rays in the energy range of  $10^1$ – $10^2$  keV. The 1L-MoS<sub>2</sub> showed a clear photoresponse to the radiation even to low dose rates down to fractions of mGy/s, showing sensitivity values up to  $2.3 \times 10^9 \mu\text{C}/\text{Gy cm}^3$ . These results promote the x-ray detectors based on 1L-MoS<sub>2</sub> as a direct competitor to the recently reported record for organic-based materials.<sup>10</sup> To improve the detector response to x rays, we exploited the already mentioned strong light–matter interaction in the visible via a scintillator film based on polydimethylsiloxane (PDMS) containing gadolinium oxysulphide doped with terbium (Gd<sub>2</sub>O<sub>2</sub>S:Tb)

was added on top of MoS<sub>2</sub>. This resulted in an increase in the photoresponse of up to three times due to the x ray to VIS spectra conversion of the scintillator. This work opens the way toward the study and production of ultrathin highly sensitive radiation detectors for real-time *in vivo* applications.

The 1L-MoS<sub>2</sub> films employed in our devices were obtained via exfoliation of a MoS<sub>2</sub> crystal. The exfoliation was performed through a thermally activated metal-mediated process. More details regarding this technique are given in previous reports<sup>36–39</sup> With this process, a MoS<sub>2</sub> monolayer was obtained on a thin gold film. The monolayer was then covered with a polystyrene (PS) film (thickness  $\sim 1 \mu\text{m}$ ) via spin coating. The gold film was etched leaving a MoS<sub>2</sub> monolayer embedded in PS. For the fabrication of the x-ray detector, the 1L-MoS<sub>2</sub> was transferred on an engineered substrate via wet transfer, leaving the PS on top of MoS<sub>2</sub> as a protective layer. The details of the wet transfer procedure are given in previous reports.<sup>36,37</sup> The device was fabricated on a soda-lime glass substrate on which gold electrodes were thermally evaporated (100 nm thickness). Anode and cathode are separated by a channel of the size of  $1 \text{ mm} \times 30 \mu\text{m}$  (channel area of  $0.03 \text{ mm}^2$ ). Figure 1(a) shows a top-view microscope picture of the device; the two black features separated in the middle are the gold anode and cathode. The MoS<sub>2</sub> monolayer flake is clearly visible and corresponds to the yellowish region. The MoS<sub>2</sub> flake has been delimited by a dashed line to simplify the recognition. The darker regions within the flake are associated with MoS<sub>2</sub> multiple layers, as already observed in previous studies.<sup>36</sup> The picture shows that the MoS<sub>2</sub> monolayer area covers the entire channel. The active area of the detector is assumed to be equal to the channel area ( $1 \times 0.03 \text{ mm}^2$ ) and its thickness is considered to be 0.9 nm, as previously observed for MoS<sub>2</sub> monolayers fabricated with this process.<sup>36</sup> The actual thickness is larger than the reported monolayer thickness (0.65 nm<sup>40</sup>) since it includes the van der Waals interaction distance between the MoS<sub>2</sub> monolayer and the substrate.

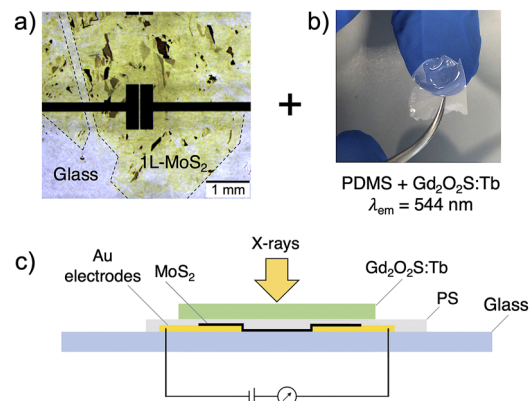


**FIG. 1.** (a) An optical image taken with a microscope of the top view of the x-ray detector device based on 1L-MoS<sub>2</sub>. The dashed line delimiting the yellow area is a guide for the eye to identify the MoS<sub>2</sub> monolayer. The two black features in the middle are the electrodes defining the active area in the channel between them. (b) An image of the scintillator film based on PDMS and loaded with Gd<sub>2</sub>O<sub>2</sub>S:Tb that is applied on top of the device. (c) A schematic cross-section of the final device exposed to x ray and connected to an external source meter unit.

To fabricate the scintillator, the following procedure was adopted: (i)  $\text{Gd}_2\text{O}_2\text{S}: \text{Tb}$  powder (UKL65/F-R1, *Phosphor Technology, Ltd.*, UK) was added (0.5 wt. %) to the base PDMS component (Bluesil<sup>TM</sup> RTV 141-a, *Elkem Silicones*, Norway), mixed, and degassed in a vacuum oven at 60 °C. (ii) The reactive PDMS component (Bluesil RTV 141-b, *Elkem Silicones*, Norway) was added in a 10:1 mass ratio with respect to the base component, followed by degassing in a vacuum oven at 60 °C. Finally, (iii) the mixture was cast via blade casting and cured at 60 °C for 4 h. A scheme of the fabrication procedure is reported in the supplementary material Fig. S1. Following these steps, a flexible and almost transparent film (0.2 mm thick) was obtained, from which the portion needed was cut [Fig. 1(b)], and finally, the scintillator was transferred on top of the PS resulting in the device whose cross section is schematically represented in Fig. 1(c).

The 1L-MoS<sub>2</sub>-based photodetector was characterized in the NUV-VIS-NIR spectrum.  $J$ - $V$  curves, temporal response, and photoresponse were measured with a device selector board (*Ossilla*, UK) connected to a Keithley 2450 source measurement unit (*Tektronix*, USA). Photoresponse in the NUV-VIS-NIR spectrum was measured under illumination with different light-emitting diodes (LEDs) (*Thorlabs*, USA). The list of the LEDs employed for this experiment with their main properties is reported in the supplementary material Table S1. The detector responsivity was calculated by normalizing the measured photocurrent with the light power illuminating the channel of the detector. The light power on the detector channel was estimated by multiplying the nominal irradiance of the LEDs at 200 mm (reported in the datasheet) with the area of the channel (0.03 mm<sup>2</sup>). In the calculation, the irradiation of the channel area was assumed to be uniform. A typical  $J$ - $V$  curve of the detector measured in dark and under illumination (455 nm, 94 μW/cm<sup>2</sup>) is reported in Fig. 2(a). The device displays low dark currents ( $\sim 10^{-1} \mu\text{A}/\text{cm}^2$ ) at  $V_{\text{bias}} < 1$  V and shows an increase in the current under light of a factor of  $\sim 10^2$ . The minimum in the dark current observed in Fig. 2(a) is shifted with respect to the zero-bias voltage. This reflects the same behavior observed in Fig. 2(c). In the graph of Fig. 2(c), the current does not return to the initial value when the light illuminating the device is switched off and the current approaches zero over a time window. The phenomenon is called persistent photoconductivity, and it has been previously observed in several studies on MoS<sub>2</sub>.<sup>41–43</sup> The photoresponse as a function of the optical power (for the 455 nm LED) is shown in Fig. 2(b). The response is found to follow an exponential dependency on the optical power ( $R \sim P^n$ ,  $n = 0.6$ ). This can be attributed to a photoconductive gain mechanism that lowers when the optical power increases.<sup>44</sup>

The dynamic of the detector was tested by measuring the current density as a function of time when the device is exposed to the illumination provided by a 455 nm LED (from 0 to 10 s) and when the light is switched off (10–20 s). The curve is reported in Fig. 2(c) and was acquired by applying a constant bias  $V_{\text{bias}}$  of 1 V. The response speed is not optimal, and the time transient is in the order of seconds. This can be associated with defects of the MoS<sub>2</sub> monolayers, mainly due to strains induced during the exfoliation and transfer procedure as well as induced by the free-standing monolayer on the electrodes. The performance is expected to improve using smoother surfaces.

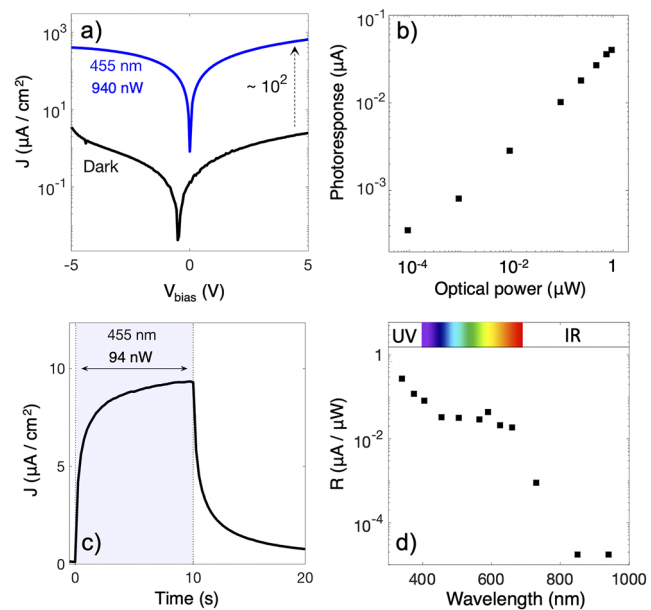


**FIG. 2.** Response of the detector based on 1L-MoS<sub>2</sub> in the near visible spectrum. (a) The  $J$ - $V$  curves measured in dark and upon illumination with a 455 nm LED are shown. (b) Photoresponse of the detector operated at 1 V as a function of the LED optical power. (c) Time evolution of the photocurrent while operating the device at 1 V by switching the LED on (0–10 s) and off (10–20 s). (d) Spectral responsivity in the NUV-VIS-NIR spectrum with the device operated at 1 V.

Responsivity of the device in the NUV-VIS-NIR spectrum, applying a bias  $V_{\text{bias}}$  of 1 V, is reported in Fig. 2(d). Although the responsivity reaches values of fractions of A/W in the NUV spectrum, it decreases to  $10^{-2}$ – $10^{-1}$  A/W in the visible range, and it drops to negligible values for IR radiation. The higher value of responsivity found around 600 nm is associated with the excitonic energy of MoS<sub>2</sub> reported that increases the absorption at that wavelength. The trend of the spectral photoresponsivity is in accordance with the absorption spectrum expected for 1L-MoS<sub>2</sub>.<sup>45</sup>

The detector was tested under x rays to demonstrate the use of MoS<sub>2</sub> as an active material for direct radiation detection. X rays were produced by a tungsten anode ( $W_{K\alpha} = 59$  keV) operated at the peak voltages of 40, 100, 150, and 195 kV filtered with 3 mm of copper. Operating the x-ray source at different peak voltages was used as a strategy to vary the dose rates over three orders of magnitudes. Dose and dose rate (dose per second) were measured with a Farmer<sup>®</sup> ionization chamber 30010/12 placed in the same position of the detector, connected to a PTW UNIDOS E electrometer (PTW, Germany), and used as a dosimetric reference for the subsequent irradiation of the detector.

The x-ray response of the 1L-MoS<sub>2</sub>-based device was measured both with and without the scintillator on top of the detector. The background arising from the irradiation of the electronics was subtracted from the measurements. The polystyrene layer on top of MoS<sub>2</sub> is estimated to absorb less than 0.01% of the x ray used in the experiment (based on data reported in Ref. 46). The measured photocurrent densities as a function of the x-ray dose rate are shown in

**Fig. 3(a)**, and the peak voltage employed during this experiment was 100 kV. The measurement of the 1L-MoS<sub>2</sub>-based device (without the scintillator) corresponds to the black markers and clearly demonstrates an x-ray response with intensity showing a linear dependency with the x-ray dose rate. This curve demonstrates, for the first time, the direct x-ray photoconversion with MoS<sub>2</sub>, showing a current density in the order of  $\mu\text{A}/\text{cm}^2$ . Similar curves and results were obtained with 40, 150, and 195 kV x rays as reported in the supplementary material Fig. S3. It was possible to measure a photoresponse down to dose rates of 0.08 mGy/s (lower dose rate limit for the irradiation setup used in this work). The response of the device was up to three times larger when adding the scintillator film based on PDMS mixed with Gd<sub>2</sub>O<sub>2</sub>S:Tb on top of the detector. The measurement is displayed in **Fig. 3(a)** by the green marks. The increased response is attributed to the additional visible photons (centered on  $\lambda = 544 \text{ nm}$ ) produced by the scintillator via indirect x-ray photoconversion. The non-linear response of the detector is associated with the non-linear output of the scintillator due to the quenching of the light emission increasing the dose rate, as previously observed for plastic scintillators.<sup>47–49</sup> The experiment was repeated by changing the voltage peak at which the x rays were generated (Fig. S3). The thin scintillator is estimated to absorb a negligible amount of x rays (less than 4%) for the energies used. Increasing the scintillator film thickness or Gd<sub>2</sub>O<sub>2</sub>S:Tb amount will lead to larger absorption and device response. Also, further engineering regarding the choice of the scintillator that maximizes the conversion efficiency and emission wavelength will lead to even larger responses. **Figure 3(b)** gives an overview of the photoresponse of the 1L-MoS<sub>2</sub>-based detector including the scintillator film for the different x-ray energies as a function of the dose rate. The highest x-ray photoresponse was obtained with x rays generated with the source at 100 kV. At similar dose rates, the response is found to increase using x-ray spectra with a lower energy distribution due to the higher x-ray attenuation of both MoS<sub>2</sub> and Gd<sub>2</sub>O<sub>2</sub>S:Tb.<sup>46</sup> The separated contributions to the signal from MoS<sub>2</sub> and scintillator varying the x-ray energy are reported in the supplementary material Fig. S4. Also, the detector showed consistent response over subsequent irradiations, indicating the reproducibility of the measurement (Fig. S5).

Finally, MoS<sub>2</sub> radiation sensitivity was calculated for different x-ray energies and dose rates to characterize the material efficiency in converting radiation into an electrical signal. The sensitivity  $S$  of a detector is calculated as the photogenerated charge (given by the time integral of the photocurrent) for unit of dose and volume, and it is expressed according to the following equation:<sup>20</sup>

$$S = \frac{\int (I_X - I_D) dt}{D \cdot V},$$

where  $I_X$ ,  $I_D$ ,  $D$ , and  $V$  represent the current recorded under x rays, the current recorded in dark conditions, the dose, and the active volume of the material, respectively. When interested in the charge collected per unit area, area sensitivity can be calculated by substituting the active volume of the detector for its active area in the equation above. The sensitivity values found are in the order of  $10^8$ – $10^9 \mu\text{C Gy}^{-1} \text{ cm}^{-3}$  (area sensitivities from  $10$  to  $10^2 \mu\text{C Gy}^{-1} \text{ cm}^{-2}$ ) with a maximum of  $2.3 \times 10^9 \mu\text{C/Gy cm}^3$  [**Fig. 3(c)**]. The sensitivity values we report may have been underestimated by up to 30%, considering that the material thickness assumed in the calculation includes the van der Walls distance between the substrate and the MoS<sub>2</sub> monolayer. These values are comparable with the record recently reported for organic-based direct x-ray detectors<sup>10</sup> and are two to three orders of magnitude higher than most of the previously reported sensitivities for direct organic and inorganic detectors.<sup>1,20</sup> Sensitivity is found to depend on the dose rate. At low dose rates, the sensitivity is higher, whereas it decreases with increasing the dose rates. This can be attributed again to an increased photoconductive gain at low dose rates due to the x-ray photogenerated carriers.

Although the findings of this study are innovative, this paper demonstrated the use of 1L-MoS<sub>2</sub> for x-ray detection in the basic scenario of an exfoliated monolayer. Challenges are now associated with the development of similar devices based on more scalable and reproducible methods to match the requirements for industrial manufacturing.

In summary, in this study, we propose TMDCs as materials for ionizing radiation detection. As proof of principle, 1L-MoS<sub>2</sub> was employed in a photodetector that showed photoresponse in a

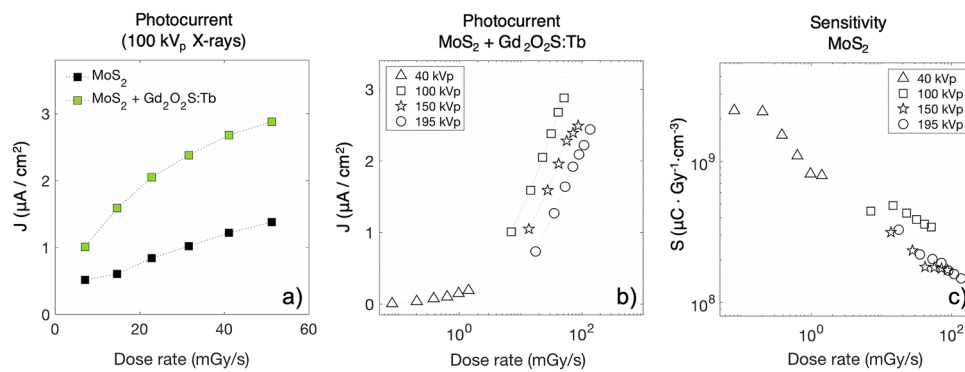


**FIG. 3.** (a) X-ray photocurrent density as a function of the x-ray dose rate operating the source at 100 kV. The black markers correspond to the 1L-MoS<sub>2</sub>-based device, while the green markers correspond to the device incorporating the scintillator film. (b) Photocurrent densities for the detector incorporating the scintillator under different x-ray energies. (c) Sensitivity of 1L-MoS<sub>2</sub> under different x-ray energies and dose rates. The detector was operated at 5 V during these measurements.

very wide range, from visible to  $10^2$  keV x rays and demonstrated, for the first time, direct photoconversion of x rays for TMDCs. MoS<sub>2</sub> showed a remarkable volume sensitivity, outperforming organic- and inorganic-based direct radiation detectors. The addition of a scintillator based on PDMS loaded with Gd<sub>2</sub>O<sub>2</sub>S:Tb was found to boost the photocurrent up to a factor of 3. This study might be an important step toward the study and production of ultrathin radiation detectors for *in vivo* applications based on TMDCs.

Supplementary material contains additional information about the production of the Gd<sub>2</sub>O<sub>2</sub>S:Tb-based scintillator films (Fig. S1), characterization of the exfoliated MoS<sub>2</sub> monolayers (Fig. S2), and further electro-optical characterization of the device (Figs. S3–S5). A table is also provided (Table S1) reporting the specifications of the LED used in the characterization of the device.

This work was performed in the frame of the program Departments of Excellence 2018–2022 (DII-UNITN)—Italian Ministry of University and Research (MIUR). The authors gratefully acknowledge the financial support by the Deutsche Forschungsgemeinschaft through CRC 951 (Project No. 182087777). The work was as well carried out in the framework of the Joint Lab GEN\_FAB and was supported by the HySPRINT Innovation Lab at Helmholtz-Zentrum Berlin.

## AUTHOR DECLARATIONS

### Conflict of Interest

The authors have no conflicts to disclose.

### Author Contributions

**Alberto Taffelli:** Conceptualization (lead); Data curation (lead); Formal analysis (lead); Investigation (lead); Methodology (lead); Validation (lead); Writing – original draft (lead); Writing – review & editing (equal). **Max Heyl:** Investigation (supporting); Writing – review & editing (supporting). **Matteo Favaro:** Investigation (supporting). **Sandra Dirè:** Methodology (supporting); Writing – review & editing (supporting). **Lucio Pancheri:** Funding acquisition (equal); Methodology (supporting); Writing – review & editing (supporting). **Emil J. W. List-Kratochvil:** Funding acquisition (equal); Methodology (supporting). **Alberto Quaranta:** Methodology (supporting); Writing – review & editing (supporting). **Giovanni Ligorio:** Investigation (supporting); Methodology (supporting); Writing – original draft (supporting); Writing – review & editing (equal).

### DATA AVAILABILITY

The data that support the findings of this study are available from the corresponding authors upon reasonable request.

### REFERENCES

- <sup>1</sup>J. A. Posar, M. Petasecca, and M. J. Griffith, “A review of printable, flexible and tissue equivalent materials for ionizing radiation detection,” *Flexible Printed Electron.* **6**(4), 043005 (2021).
- <sup>2</sup>G. Pipan, M. Bogar, A. Ciavatti, L. Basiricò, T. Cramer, B. Fraboni, and A. Fraleoni-Morgera, “Direct inkjet printing of TIPS-pentacene single crystals onto interdigitated electrodes by chemical confinement,” *Adv. Mater. Interfaces* **5**(3), 1700925 (2018).
- <sup>3</sup>L. Basiricò, A. Ciavatti, T. Cramer, P. Cosseddu, A. Bonfiglio, and B. Fraboni, “Direct X-ray photoconversion in flexible organic thin film devices operated below 1 V,” *Nat. Commun.* **7**, 13063 (2016).
- <sup>4</sup>D. Zhao, M. Xu, B. Xiao, B. Zhang, L. Yan, G. Zeng, A. Dubois, P. Sellin, W. Jie, and Y. Xu, “Purely organic 4HCB single crystals exhibiting high hole mobility for direct detection of ultralow-dose X-radiation,” *J. Mater. Chem. A* **8**(10), 5217–5226 (2020).
- <sup>5</sup>A. Ciavatti, E. Capria, A. Fraleoni-Morgera, G. Tromba, D. Dreossi, P. J. Sellin, P. Cosseddu, A. Bonfiglio, and B. Fraboni, “Toward low-voltage and bendable X-ray direct detectors based on organic semiconducting single crystals,” *Adv. Mater.* **27**(44), 7213–7220 (2015).
- <sup>6</sup>B. Fraboni, A. Ciavatti, F. Merlo, L. Pasquini, A. Cavallini, A. Quaranta, A. Bonfiglio, and A. Fraleoni-Morgera, “Organic semiconducting single crystals as next generation of low-cost, room-temperature electrical X-ray detectors,” *Adv. Mater.* **24**(17), 2289–2293 (2012).
- <sup>7</sup>F. A. Boroumand, M. Zhu, A. B. Dalton, J. L. Keddie, P. J. Sellin, and J. J. Gutierrez, “Direct x-ray detection with conjugated polymer devices,” *Appl. Phys. Lett.* **91**(3), 033509 (2007).
- <sup>8</sup>J. A. Posar, J. Davis, M. J. Large, L. Basiricò, A. Ciavatti, B. Fraboni, O. Dhez, D. Wilkinson, P. J. Sellin, M. J. Griffith, M. L. F. Lerch, A. Rosenfeld, and M. Petasecca, “Characterization of an organic semiconductor diode for dosimetry in radiotherapy,” *Med. Phys.* **47**(8), 3658–3668 (2020).
- <sup>9</sup>P. Büchele, M. Richter, S. F. Tedde, G. J. Matt, G. N. Anka, R. Fischer, M. Biele, W. Metzger, S. Lilliu, O. Bikondoa, J. E. Macdonald, C. J. Brabec, T. Kraus, U. Lemmer, and O. Schmidt, “X-ray imaging with scintillator-sensitized hybrid organic photodetectors,” *Nat. Photonics* **9**(12), 843–848 (2015).
- <sup>10</sup>I. Temiño, L. Basiricò, I. Fratelli, A. Tamayo, A. Ciavatti, M. Mas-Torrent, and B. Fraboni, “Morphology and mobility as tools to control and unprecedentedly enhance X-ray sensitivity in organic thin-films,” *Nat. Commun.* **11**(1), 2136 (2020).
- <sup>11</sup>Y. Zhang, Y. Liu, Z. Xu, H. Ye, Z. Yang, J. You, M. Liu, Y. He, M. G. Kanatzidis, and S. F. Liu, “Nucleation-controlled growth of superior lead-free perovskite Cs<sub>3</sub>Bi<sub>2</sub>I<sub>9</sub> single-crystals for high-performance X-ray detection,” *Nat. Commun.* **11**(1), 2304 (2020).
- <sup>12</sup>W. Pan, H. Wu, J. Luo, Z. Deng, C. Ge, C. Chen, X. Jiang, W. J. Yin, G. Niu, L. Zhu, L. Yin, Y. Zhou, Q. Xie, X. Ke, M. Sui, and J. Tang, “Cs<sub>2</sub>AgBiBr<sub>6</sub> single-crystal X-ray detectors with a low detection limit,” *Nat. Photonics* **11**(11), 726–732 (2017).
- <sup>13</sup>J. Liu, B. Shabbir, C. Wang, T. Wan, Q. Ou, P. Yu, A. Tadich, X. Jiao, D. Chu, D. Qi, D. Li, R. Kan, Y. Huang, Y. Dong, J. Jasieniak, Y. Zhang, and Q. Bao, “Flexible, printable soft-X-ray detectors based on all-inorganic perovskite quantum dots,” *Adv. Mater.* **31**(30), 1901644 (2019).
- <sup>14</sup>A. Ciavatti, R. Sorrentino, L. Basiricò, B. Passarella, M. Caironi, A. Petrozza, and B. Fraboni, “High-sensitivity flexible X-ray detectors based on printed perovskite Inks,” *Adv. Funct. Mater.* **31**(11), 2009072 (2021).
- <sup>15</sup>M. Bruzzi and C. Talamonti, “Characterization of crystalline CsPbBr<sub>3</sub> perovskite dosimeters for clinical radiotherapy,” *Front. Phys.* **9**, 625282 (2021).
- <sup>16</sup>M. Hu, S. Jia, Y. Liu, J. Cui, Y. Zhang, H. Su, S. Cao, L. Mo, D. Chu, G. Zhao, K. Zhao, Z. Yang, and S. F. Liu, “Large and dense organic-inorganic hybrid perovskite CH<sub>3</sub>NH<sub>3</sub>PbI<sub>3</sub> wafer fabricated by one-step reactive direct wafer production with high X-ray sensitivity,” *ACS Appl. Mater. Interfaces* **12**(14), 16592–16600 (2020).
- <sup>17</sup>H. Wei, D. Desantis, W. Wei, Y. Deng, D. Guo, T. J. Savenije, L. Cao, and J. Huang, “Dopant compensation in alloyed CH<sub>3</sub>NH<sub>3</sub>PbBr<sub>3-x</sub>Cl<sub>x</sub> perovskite single crystals for gamma-ray spectroscopy,” *Nat. Mater.* **16**(8), 826–833 (2017).
- <sup>18</sup>W. Wei, Y. Zhang, Q. Xu, H. Wei, Y. Fang, Q. Wang, Y. Deng, T. Li, A. Gruber, L. Cao, and J. Huang, “Monolithic integration of hybrid perovskite single crystals with heterogenous substrate for highly sensitive X-ray imaging,” *Nat. Photonics* **11**(5), 315–321 (2017).
- <sup>19</sup>H. Wei, Y. Fang, P. Mulligan, W. Chuirazzi, H. H. Fang, C. Wang, B. R. Ecker, Y. Gao, M. A. Loi, L. Cao, and J. Huang, “Sensitive X-ray detectors made of methylammonium lead tribromide perovskite single crystals,” *Nat. Photonics* **10**(5), 333–339 (2016).
- <sup>20</sup>H. M. Thirimanse, K. D. G. I. Jayawardena, A. J. Parnell, R. M. I. Bandara, A. Karalasingam, S. Pani, J. E. Huerdler, D. G. Lidzey, S. F. Tedde, A. Nisbet, C. A.

- Mills, and S. R. P. Silva, "High sensitivity organic inorganic hybrid X-ray detectors with direct transduction and broadband response," *Nat. Commun.* **9**(1), 2926 (2018).
- <sup>21</sup>J. H. Noh, S. H. Im, J. H. Heo, T. N. Mandal, and S. I. Seok, "Chemical management for colorful, efficient, and stable inorganic–organic hybrid nanostructured solar cells," *Nano Lett.* **13**(4), 1764–1769 (2013).
- <sup>22</sup>S. Emami, L. Andrade, and A. Mendes, "Recent progress in long-term stability of perovskite solar cells," *U Porto J. Eng.* **1**(2), 52–62 (2015).
- <sup>23</sup>K. L. Kovalenko, S. I. Kozlovskiy, and N. N. Sharan, "Electron mobility in molybdenum disulfide: From bulk to monolayer," *Phys. Status Solidi B* **257**(5), 1900635 (2020).
- <sup>24</sup>H. Ji, G. Lee, M. K. Joo, Y. Yun, H. Yi, J. H. Park, D. Suh, and S. C. Lim, "Thickness-dependent carrier mobility of ambipolar MoTe<sub>2</sub>: Interplay between interface trap and Coulomb scattering," *Appl. Phys. Lett.* **110**(18), 183501 (2017).
- <sup>25</sup>A. Rawat, N. Jena, Dimple, and A. De Sarkar, "A comprehensive study on carrier mobility and artificial photosynthetic properties in Group VI B transition metal dichalcogenide monolayers," *J. Mater. Chem. A* **6**(18), 8693–8704 (2018).
- <sup>26</sup>S. Jo, N. Ubrig, H. Berger, A. B. Kuzmenko, and A. F. Morpurgo, "Mono- and bilayer WS<sub>2</sub> light-emitting transistors," *Nano Lett.* **14**, 2019 (2014).
- <sup>27</sup>A. Splendiani, L. Sun, Y. Zhang, T. Li, J. Kim, C. Y. Chim, G. Galli, and F. Wang, "Emerging photoluminescence in monolayer MoS<sub>2</sub>," *Nano Lett.* **10**(4), 1271–1275 (2010).
- <sup>28</sup>K. K. Kam and B. A. Parkinson, "Detailed photocurrent spectroscopy of the semiconducting group VIB transition metal dichalcogenides," *J. Phys. Chem.* **86**(4), 463–467 (1982).
- <sup>29</sup>M. Bernardi, M. Palummo, and J. C. Grossman, "Extraordinary sunlight absorption and one nanometer thick photovoltaics using two-dimensional monolayer materials," *Nano Lett.* **13**(8), 3664–3670 (2013).
- <sup>30</sup>J. Y. Kwak, "Absorption coefficient estimation of thin MoS<sub>2</sub> film using attenuation of silicon substrate Raman signal," *Results Phys.* **13**, 102202 (2019).
- <sup>31</sup>D. S. Tsai, D. H. Lien, M. L. Tsai, S. H. Su, K. M. Chen, J. J. Ke, Y. C. Yu, L. J. Li, and J. H. He, "Trilayered MoS<sub>2</sub> metal -semiconductor-metal photodetectors: Photogain and radiation resistance," *IEEE J. Sel. Top. Quantum Electron.* **20**(1), 30–35 (2014).
- <sup>32</sup>A. J. Arnold, T. Shi, I. Jovanovic, and S. Das, "Extraordinary radiation hardness of atomically thin MoS<sub>2</sub>," *ACS Appl. Mater. Interfaces* **11**(8), 8391–8399 (2019).
- <sup>33</sup>J. Gao, B. Li, J. Tan, P. Chow, T. M. Lu, and N. Koratkar, "Aging of transition metal dichalcogenide monolayers," *ACS Nano* **10**(2), 2628–2635 (2016).
- <sup>34</sup>H. S. Nalwa, "A review of molybdenum disulfide (MoS<sub>2</sub>) based photodetectors: From ultra-broadband, self-powered to flexible devices," *RSC Adv.* **10**(51), 30529–30602 (2020).
- <sup>35</sup>A. Taffelli, S. Dirè, A. Quaranta, L. Pancheri, and G. Villanueva, "MoS<sub>2</sub> based photodetectors: A review," *Sensors* **21**, 2758 (2021).
- <sup>36</sup>M. Heyl, D. Burmeister, T. Schultz, S. Pallasch, G. Ligorio, N. Koch, and E. J. W. List-Kratochvil, "Thermally activated gold-mediated transition metal dichalcogenide exfoliation and a unique gold-mediated transfer," *Phys. Status Solidi* **14**(11), 2000408 (2020).
- <sup>37</sup>M. Heyl, S. Grützmacher, S. Rühl, G. Ligorio, N. Koch, and E. J. W. List-Kratochvil, "Low temperature heating of Silver-mediated exfoliation of MoS<sub>2</sub>," *Adv. Mater. Interfaces* **9**, 2200362 (2022).
- <sup>38</sup>M. Heyl and E. J. W. List-Kratochvil, "Only gold can pull this off: Mechanical exfoliations of transition metal dichalcogenides beyond scotch tape," *Appl. Phys. A* **129**(1), 16 (2023).
- <sup>39</sup>S. Grützmacher, M. Heyl, N. M. Vittorio, K. Norbert, E. J. W. List-Kratochvil, and G. Ligorio, "Local manipulation of the energy levels of 2D TMDCs on the microscale level via microprinted self-assembled monolayers," *Adv. Mater. Interfaces* **10**, 2300276 (2023).
- <sup>40</sup>X. Li and H. Zhu, "Two-dimensional MoS: Properties, preparation, and applications," *J. Mater.* **1**(1), 33–44 (2015).
- <sup>41</sup>Y. C. Wu, C. H. Liu, S. Y. Chen, F. Y. Shih, P. H. Ho, C. W. Chen, C. T. Liang, and W. H. Wang, "Extrinsic origin of persistent photoconductivity in monolayer MoS<sub>2</sub> field effect transistors," *Sci. Rep.* **5**, 11472 (2015).
- <sup>42</sup>A. Di Bartolomeo, L. Genovese, T. Foller, F. Giubileo, G. Luongo, L. Croin, S. J. Liang, L. K. Ang, and M. Schleberger, "Electrical transport and persistent photoconductivity in monolayer MoS<sub>2</sub> phototransistors," *Nanotechnology* **28**(21), 214002 (2017).
- <sup>43</sup>A. George, M. V. Fistul, M. Gruenewald, D. Kaiser, T. Lehnert, R. Mupparapu, C. Neumann, U. Hübner, M. Schaal, N. Masurkar, L. M. R. Arava, I. Staude, U. Kaiser, T. Fritz, and A. Turchanin, "Giant persistent photoconductivity in monolayer MoS<sub>2</sub> field-effect transistors," *npj 2D Mater. Appl.* **5**(1), 15 (2021).
- <sup>44</sup>M. M. Furchi, D. K. Polyushkin, A. Pospischil, and T. Mueller, "Mechanisms of photoconductivity in atomically thin MoS<sub>2</sub>," *Nano Lett.* **14**(11), 6165 (2014).
- <sup>45</sup>K. P. Dhakal, D. L. Duong, J. Lee, H. Nam, M. Kim, M. Kan, Y. H. Lee, and J. Kim, "Confocal absorption spectral imaging of MoS<sub>2</sub>: Optical transitions depending on the atomic thickness of intrinsic and chemically doped MoS<sub>2</sub>," *Nanoscale* **6**(21), 13028 (2014).
- <sup>46</sup>See <https://physics.nist.gov/PhysRefData/XrayMassCoef/chap2.html> for NIST: X-ray mass attenuation coefficients.
- <sup>47</sup>J. B. Birks, "Scintillations from organic crystals: Specific fluorescence and relative response to different radiations," *Proc. Phys. Soc. Sect. A* **64**(10), 874–877 (1951).
- <sup>48</sup>K. Wick, D. Paul, P. Schröder, V. Stieber, and B. Bicken, "Recovery and dose rate dependence of radiation damage in scintillators, wavelength shifters and light guides," *Nucl. Instrum. Methods Phys. Res. Sect. B* **61**(4), 472–486 (1991).
- <sup>49</sup>E. Biagtan, E. Goldberg, R. Stephens, E. Valeroso, and J. Harmon, "Gamma dose and dose rate effects on scintillator light output," *Nucl. Instrum. Methods Phys. Res. Sect. B* **108**(1–2), 125–128 (1996).